ELSEVIER

Nuclear Instruments and Methods in Physics Research A 453 (2000) 289–295

NUCLEAR INSTRUMENTS & METHODS IN PHYSICS RESEARCH Section A

www.elsevier.nl/locate/nima

The HERA-B RICH

I. Ariño[b], J. Bastos[c], D. Broemmelsiek[d], J. Carvalho[c], P. Conde[b], D. Dujmić[a], R. Eckmann[a], L. Garrido[b], A. Gorišek[g], I. Ivaniouchenkov[c], M. Ispirian[f], S. Karabekian[e], S. Korpar[g], P. Križan[g,*], K. Lau[f], R. Miquel[b], D. Peralta[b], R. Pestotnik[g], J. Pyrlik[f], D. Ramachandran[f], K. Reeves[a], J. Rosen[d], R.F. Schwitters[a], M. Starič[g], A. Stanovnik[g], D. Škrk[g], T. Živko[g]

[a]*University of Texas, Austin, USA*
[b]*University of Barcelona, Spain*
[c]*LIP Coimbra, Portugal*
[d]*Northwestern University, Evanston, USA*
[e]*DESY, Hamburg, Germany*
[f]*University of Houston, Houston, USA*
[g]*J. Stefan Institute and University of Ljubljana, P.O. Box 100, Jadranska 19, 61000 Ljubljana, Slovenia*

Accepted 19 June 2000

Abstract

The design issues and tests carried out with the ring imaging Cherenkov detector for the HERA-B experiment are reviewed. Results of on-the-bench tests of the employed photomultiplier tubes are reported together with the early commissioning measurements with the HERA proton beam.

Keywords: Ring imaging; Cherenkov detectors; Photomultiplier tubes; HERA-B

1. Introduction

The HERA-B experiment [1] aims at measuring: CP violation in $B^0 \to J/\psi K^0_S$ and $B^0 \to \pi^+\pi^-$ decays, $B^0_s\bar{B}^0_s$ mixing and $B\bar{B}$ decays with two leptons in the final state. The B mesons will be produced in collisions of 920 GeV/c protons with a fixed target. The target consists of 8 wires in the halo of the proton beam in order not to disturb experiments measuring ep collisions. One of the essential components of the spectrometer is the ring imaging counter [1–3]. In what follows we shall describe the essential components of the counter, and will then present the results of the commissioning phase.

2. The HERA-B RICH

The main purpose of the Ring Imaging Cherenkov counter (RICH) in the HERA-B experiment is the tagging of the B meson flavour. Tagging of the B^0 or the $\bar{B}^0$ meson is accomplished by identifying the charged kaon into which the associated B meson decayed. Identifying the charged kaon

* Corresponding author.
E-mail address: peter.krizan@ijs.si (P. Križan).

0168-9002/00/$ - see front matter
PII: S0168-9002(00)00647-1

essentially means separating it from the pion between 3 GeV/c and about 50 Gev/c at an interaction rate of 40 MHz.

Perfluorobutane gas (C_4F_{10}) has been chosen for the HERA-B RICH radiator, since it combines a relatively high refractive index and low dispersion. In this gas the Cherenkov radiation threshold momenta for pions and kaons are at 2.7 and 9.6 GeV/c, respectively. For $\beta = 1$ particles, the Cherenkov angle is 51.5 mrad, while the $\pi - K$ difference in Cherenkov angle is 0.9 mrad at 50 GeV/c. The set-up of the counter is schematically shown in Fig. 1. The two spherical mirror halves are tilted, i.e. the center of curvature of each mirror half is displaced relative to the target position. Cherenkov photons are thus reflected to photon detectors well outside the charged particle flux.

The 108 m^3 vessel for the C_4F_{10} gas radiator has been constructed from stainless steel, except for the particle entry and exit windows (1 mm Al) and the photon exit windows (UVT perspex). Also, two beam shrouds close the gas volume around the two beam pipes for protons and electrons. The purification and circulation system for the C_4F_{10} gas has been constructed at CERN and was commissioned at DESY. It is worth noting that the initial filling of the volume amounts to about 1100 kg of C_4F_{10}.

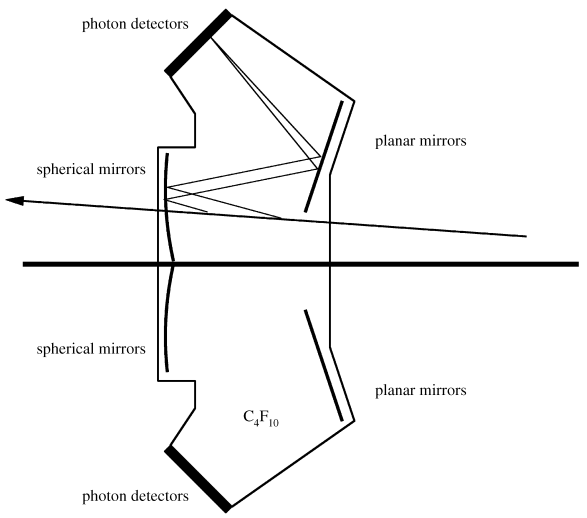

Fig. 1. The HERA-B RICH.

Two mirror systems, a spherical and a planar one, are made of hexagonal and rectangular units, respectively. The hexagonal mirror segments with 11.4 m radius of curvature have been produced from 7 mm thick grinded glass. The mirror quality has been determined upon delivery by measuring for each segment the radius of curvature, and the fraction of reflected light, as well as by recording a Ronchi image to check the homogeneity of the mirror surface. The reflectivity was required to exceed 85% in the wavelength interval 250–600 nm. Each spherical mirror segment is supported at three points, two of which can be moved, and are motor driven via a transmission mechanism with a feed through to the exterior of the vessel. The planar mirrors are made of float glass, thus being significantly cheaper at the required optical quality. By making use of the data gathered on all the mirror segments, it was possible to group them in the tiling scheme according to their optical quality and resolution requirements [4].

3. Photon detector

The photon detector consists of Hamamatsu multianode R5900 M16 and M4 photomultiplier tubes. The M16 version has 16 pads of 4.5×4.5 mm^2 each, with a 12-stage, metal-foil dynode system [5]. The M4 version has 4 pads of 9×9 mm^2 each, and 10 dynodes. The quantum efficiency of the photocathode with borosilicate window has a broad plateau in the wavelength region between 300 nm and 500 nm with a maximum value of 20%. The UV-extended version has a UV transparent window, which shifts the low wavelength cut-off to about 250 nm. The other PM characteristics such as the required cathode high voltage (≤ 1000 V), the current amplification (10^7), dark current (~ 1 nA), pulse rise time (0.8 ns), transit time spread (0.3 ns) [5], are also satisfactory.

The outer dimensions of the PMT are 28×28 mm^2, so the photocathode occupies only about 30% of the surface. Due to the smaller photocathode surface compared to the photomultiplier cross-section, a two-lens demagnification system (2:1) was designed (Fig. 2) [6,7]. The lenses are made of UVT perspex with high transparency

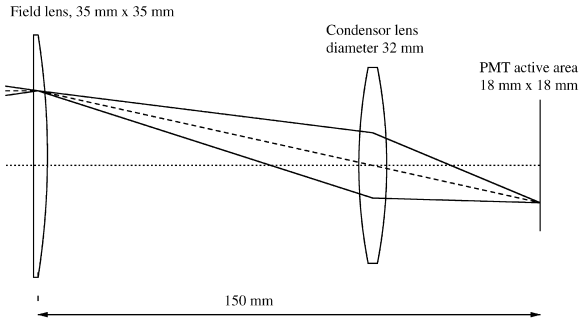

Fig. 2. The optical system for light collection and demagnification. The two rays shown in full line correspond to photons with incident angles of $\pm$ 100 mrad.

over most of the wavelength region where the photocathode is sensitive. The angular acceptance of the optical system is also satisfactory and is uniform for incident angles below about 110 mrad [8]. In addition to increasing the active area the lens system also adjusts the required pixel size in the central detector region (9×9 mm^2) to the PMT pad size 4.5×4.5 mm^2. The outer detector region with lower occupancy and looser resolution requirements uses the M4 version of the tube with two times larger pads (9×9 mm^2) with the same lens system, such that the pixel size amounts to 18×18 mm^2.

Four PMTs are positioned on a common base board, which houses the voltage divider, signal lines and the front-end electronics consisting of 16-channel boards based on the ASD8 chip [9]. In Fig. 3 a photograph of a fully equipped basic module for the M16 photomultiplier tubes is presented.

In order to reduce the contribution of spherical aberration to the overall resolution of the Cherenkov angle, an optimal surface of the Cherenkov photon detector has been calculated [10–12]. Each half-detector (upper and lower) consists of 5 flat supermodules placed in order to approximate the optimal surface, which is close to the shape of a flattened (ellipsoidal) cylinder. Such an arrangement also ensures better acceptance for the Cherenkov photons, which should be incident onto the flat supermodules at angles below 110 mrad.

From the data available on the quantum efficiency [5], mirror reflectivities [4], window and optical system transmissions [6,7], one calculates the merit

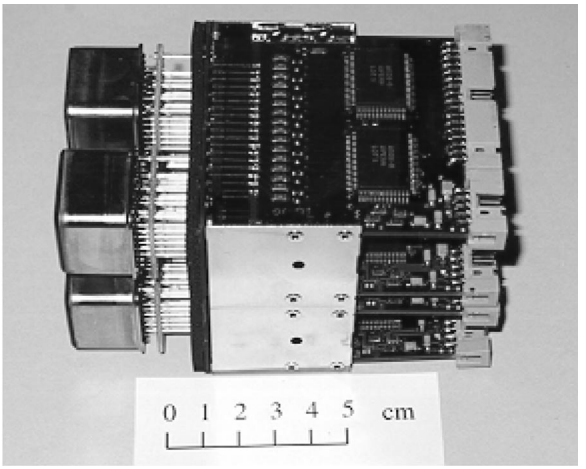

Fig. 3. Fully equipped photomultiplier basic module housing Hamamatsu R5900 photomultiplier tubes type M16.

factor $N_0 = 43$ cm^{-1}, such that the expected number of photons for particles approaching the velocity of light amounts to $N_{\mathrm{det}} = N_0 L \sin^2 \vartheta = 31$ with $L = 2.7$ m and $\vartheta = 51.5$ mrad. The expected single-photon resolution is 0.7 and 1 mrad for the regions occupied by M16 and M4 PMTs, respectively.

4. Measurements and results

4.1. On-the-bench tests

In the initial set of measurements [13] the single-photon counting properties of the photomultiplier tube were investigated, in particular the efficiency for single-photon detection as well as the background count rate. It was established that the tube allows for a good single photoelectron detection, with good uniformity (Fig. 4), very little cross talk and low background count rate.

Tests of all the 2305 PMTs (1543 M16s and 762 M4s) have been made in the laboratory prior to the installation in the photon detector [14]. Cherenkov photons produced by β electrons of a ^{90}Sr source were used as a stable light source. Four tubes were tested at the same time, of which one was used as a reference. For each photomultiplier tube, the source and background rates were recorded as

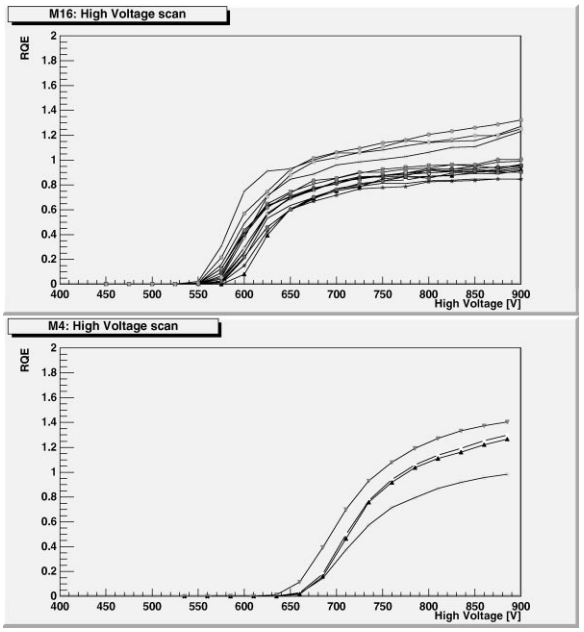

Fig. 4. Dependence of a suitably normalized rate as a function of the high voltage for all channels of a representative M16 (above) and M4 (below) photomultiplier tube.

a function of high voltage and threshold setting. On the basis of these tests, the photomultipliers have been grouped according to similar high-voltage characteristics, allowing all PMTs within a group to be connected to the same high voltage, thus maximising the efficiency for the given, much smaller number of independent HV channels [15]. The results obtained for the optimal high voltage as well as for the relative PMT sensitivity were compared to values provided by the manufacturer, and a good agreement was found [16].

The count rates of the reference M4 and M16 photomultipliers were recorded during the quality assessment tests, and were also continually measured after the tests were finished, in order to obtain an estimate of the long term stability. The count rate decrease in two years is consistent with the known decay rate of the ^{90}Sr source.

4.2. Test measurements in situ

With the photon detectors in their proper position in the HERA-B spectrometer, the photo-

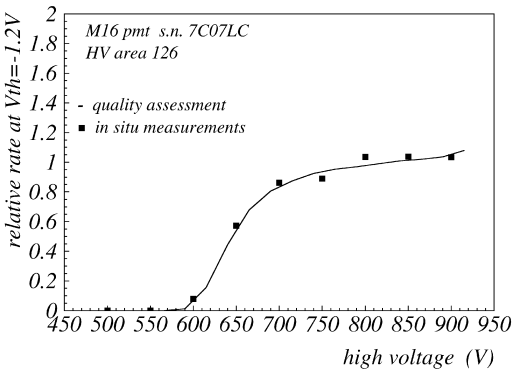

Fig. 5. The plateau curve for a typical M16 tube. The data labelled "in situ" represent values measured during the photon detector testing in its final position, while the curves labelled "quality assessment" correspond to measurements made in the laboratory during on-the-bench quality tests. The two sets of data are normalised to the average of the three points at 750, 800 and 850 V.

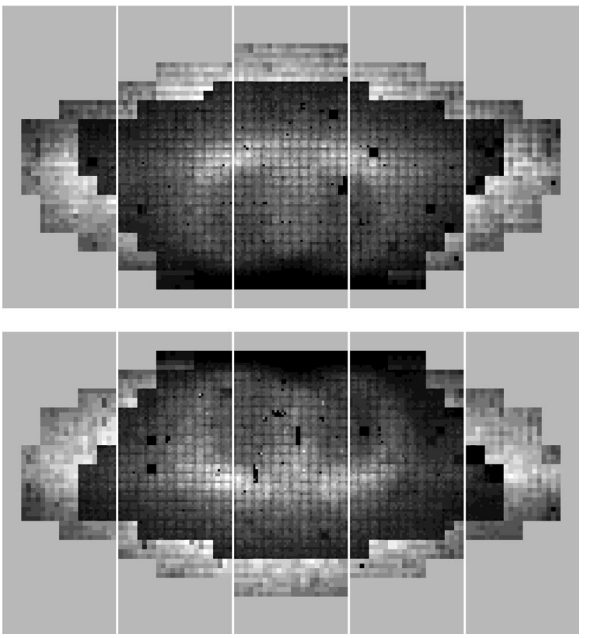

Fig. 6. The occupancy of the upper and lower photon detectors shows the region occupied by M16 (inner region) and M4 PMTs (outer region). The peak values, shown in white, correspond to rates around 1.5 MHz per channel.

multipliers cabled to the readout system and with freon as Cherenkov radiator, the commissioning of the system became possible. Fig. 5 gives the count rate versus high voltage for a representative

photomultiplier. It is seen that the curves measured in situ with the HERA proton beam agree nicely with the ^{90}Sr source measurements. The occupancy is shown in Fig. 6, where the region occupied by M16 PMTs is clearly distinguished from the region occupied by M4 PMTs. We also note that only about 0.3% of the nearly 30.000 channels were found to be noisy, and were excluded from further analysis.

Due to non-availability of information from the particle tracking system, the Cherenkov ring radii were deduced by finding the rings which best fit the detected hits on the photon detector. Only events which depict well separated Cherenkov rings were employed in a simple analysis [17]. In the analysis one counts the detected photons per Cherenkov ring by looking at appropriate events (one of which is shown in Fig. 7) and measures the corresponding ring radius. The number of counted hits per Cherenkov ring is plotted as a function of Cherenkov angle in Fig. 8. The lines drawn on the plot correspond to a hypothesis that $31 \pm \sqrt{31}$ photons are radiated from particles approaching the velocity of light. For each of the rings recorded in Fig. 8, we calculated the photon detector response parameter N_0. The resulting distribution is shown in Fig. 9. We observe that the average value of the photon detector response parameter as well as the average number of detected photons per ring are consistent with expectations.

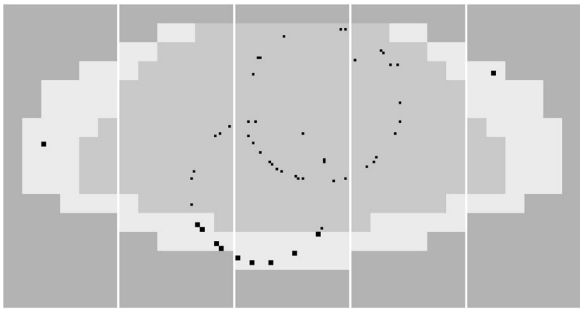

Fig. 7. Two intersecting Cherenkov rings, one with 22 photons detected by 4- and 16-channel photomultiplier tubes, a measured Cherenkov angle of 45.5 ± 0.5 mrad and expected number of 23.8 ± 1.5 hits, and a ring with 27 photons detected exclusively by 16-channel photomultiplier tubes, 49.8 ± 0.5 mrad Cherenkov angle and expected 28.5 ± 1.8 hits.

RICH can, in absence of the main tracking system, serve as a stand-alone tracking device [18]. From the rings found on the photon detector, track directions are deduced, and matched in the non-bending plane with the track candidates from the silicon vertex detector. From the deflection in the bending plane the momentum of the particle is then determined. The resulting identification capabilities are shown in Fig. 10. We also note that the resolution as determined from the stand-alone ring search analysis [19] is consistent with the design values of 0.7 and 1 mrad for M16 and M4 PMTs.

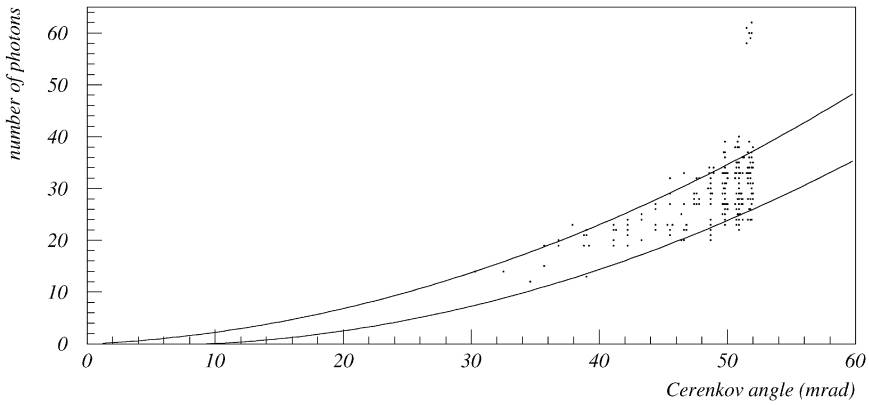

Fig. 8. Measured (data points) and expected ($\pm \sigma$ curves) number of detected photons versus Cherenkov angle for nearly 200 rings which could be well separated. Some events are also seen with two times more detected photons per ring than expected. They are due to Cherenkov radiation of an overlapping e^+e^- pair.

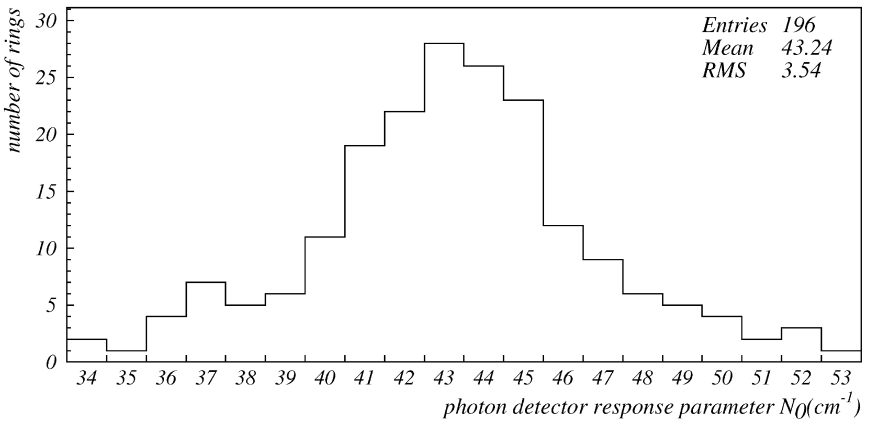

Fig. 9. The distribution of the photon detector response parameter N_0.

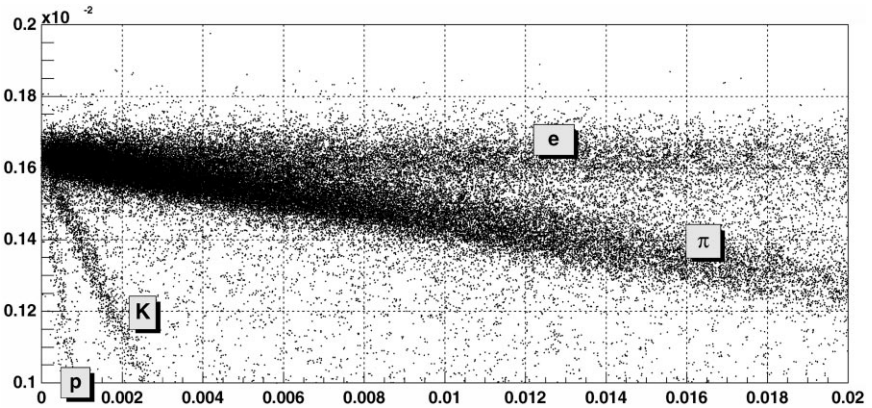

Fig. 10. Identification capabilities without the final tracking system: the correlation between the Cherenkov angle squared (in rad^2, vertical axis) and inverse momentum squared (in $(\mathrm{GeV}/c)^{-2}$, horizontal axis). For a given mass a linear relation between the two is expected. Note that a mixture of freon and nitrogen with a saturated Cherenkov angle of 41 mrad was used as the radiator gas.

5. Summary

A ring imaging Cherenkov counter for a high rate environment of the HERA-B experiment was designed, tested, installed and commissioned. A preliminary data analysis shows that the two critical parameters, the figure of merit $N_0 = 43\ \mathrm{cm}^{-1}$, resulting in 31 detected photons on a saturated Cherenkov ring, and the single-photon resolution of 0.7–1.0 mrad, are close to the design values.

References

[1] T. Lohse et al., Proposal for HERA-B, DESY PRC-94/02, May 1994.
[2] J.L. Rosen, Nucl. Instr. and Meth. A 408 (1998) 191.
[3] S. Korpar et al., Nucl. Instr. and Meth. A 433 (1999) 128.
[4] D. Dujmić, K. Reeves, HERA-B RICH Note 97-182, Hamburg, 1997.
[5] Hamamatsu Data Sheets for R5900-M16 and R5900-M4 Photomultipliers.
[6] J. McGill, R. Schwitters, HERA-B Note 96-278, DESY, Hamburg, 1996.
[7] D. Broemmelsiek, Nucl. Instr. and Meth. A 433 (1999) 136.

[8] R. Eckmann, M. Ispirian, S. Karabekyan, J. McGill, R. Schwitters, HERA-B Note 97-162, DESY, Hamburg, 1997.
[9] F.M. Newcomer et al., IEEE Trans. Nucl. Sci. 40 (4) (1993) 630.
[10] P. Križan, M. Starič, Nucl. Instr. and Meth. A 379 (1996) 124.
[11] R. Schwitters, HERA-B Note 97-088, DESY, Hamburg, 1997.
[12] D. Dujmić, R. Schwitters, HERA-B Note 98-052, DESY, Hamburg, 1998.
[13] P. Križan, S. Korpar, R. Pestotnik, M. Starič, A. Stanovnik, E. Michel, C. Oehser, W. Schmidt-Parzefall, A. Schwarz, T. Hamacher, D. Broemmelsiek, J. Pyrlik, Nucl. Instr. and Meth. A 394 (1997) 27.
[14] S. Korpar et al., Nucl. Instr. and Meth. A 442 (2000) 316.
[15] J. Pyrlik, K. Lau, HERA-B Note 97-182, DESY, Hamburg, 1997.
[16] S. Korpar, R. Pestotnik, P. Križan, IJS Report, IJS-DP-7615, Ljubljana, 1997: HERA-B Note 97-079, DESY, Hamburg, 1997.
[17] D. Škrk, Doctoral Thesis, Univerza v Ljubljani, Fakulteta za matematiko in fiziko, Oddelek za fiziko, Ljubljana, June 1999.
[18] D. Dujmić, R. Eckmann, K. Reeves, R.F. Schwitters, HERA-B Note 99-100, DESY, Hamburg, 1999.
[19] R. Schwitters, HERA-B Note 99-215, DESY, Hamburg, 1999.